Available online at www.sciencedirect.com
SCIENCE DIRECT
Sensors and Actuators A 123–124 (2005) 326–330
SENSORS AND ACTUATORS A PHYSICAL
www.elsevier.com/locate/sna

Image and color recognition using amorphous silicon p–i–n photodiodes

Paula Louro [a,*], Manuela Vieira [a], Alessandro Fantoni [a], Miguel Fernandes [a], C. Nunes de Carvalho [b], G. Lavareda [c]

[a] *DEETC, ISEL, R. Conselheiro Emídio Navarro 1, 1900-014 Lisbon, Portugal*
[b] *C1, IST, Av. Rovisco Pais, 1049-001 Lisboa, Portugal*
[c] *DCM, FCT-UNL, Quinta da Torre, 2829-516 Caparica, Portugal*

Received 13 September 2004; received in revised form 2 March 2005; accepted 4 March 2005
Available online 12 May 2005

Abstract

Large area hydrogenated amorphous silicon single and stacked p–i–n structures with low conductivity doped layers are proposed as monochrome and color image sensors. The layers of the structures are based on amorphous silicon alloys (a-Si_xC_{1-x}:H). The current–voltage characteristics and the spectral sensitivity under different bias conditions are analyzed. The output characteristics are evaluated under different read-out voltages and scanner wavelengths. To extract information on image shape, intensity and color, a modulated light beam scans the sensor active area at three appropriate bias voltages and the photoresponse in each scanning position ("sub-pixel") is recorded. The investigation of the sensor output under different scanner wavelengths and varying electrical bias reveals that the response can be tuned, thus enabling color separation. The operation of the sensor is exemplified and supported by a numerical simulation.

Category: 4 (Non-magnetic physical devices); 10 (Applications)

Keywords: Photodiode; Image sensor; Color detection

1. Introduction

Image sensing device is an apparatus for transforming light image into a sequential electronic signal. They are usually based on arrays of sensing elements. They capture light on a grid of small pixels on their surfaces and image sensing is performed using two basic techniques: line scanning and area scanning [1,2].

Resolution is not the only factor governing the quality of the images. Equally important is the color. Silicon based devices are monochrome in nature. Color image processing is usually performed with the aid of three-color sequential filters or integral color filter arrays overlaying the devices. In this respect, voltage bias controlled color detection by two-terminal thin film devices is very interesting since one instead of three or four pixels will be sufficient for color discrimination, there is a remarkable gain in spatial resolution, and color filters as a major cost driver are no longer needed.

Various structures and sequences have been suggested [3–6]. In our group, efforts have been devoted towards the development of a new kind of image sensor [7,8]. This sensor consists on one large cell detector or pixel (picture element) where the optical image is scanned by sequentially detecting scene information at discrete *XY* coordinates. The read-out of the injected carriers is achieved by measuring the ac component of the current, i_{ac}.

For simultaneous image and color detection the wavelength filtering property of the silicon has to be combined with the sensor responsivity dependence on the applied voltage. This work intends to evaluate the possibility of color selectivity in single and stacked large area p–i–n cells by controlling parameters like scanner wavelength and read-out

* Corresponding author. Tel.: +351 21 8317290; fax: +351 21 8317114.
E-mail address: plouro@deetc.isel.ipl.pt (P. Louro).

0924-4247/$ – see front matter © 2005 Elsevier B.V. All rights reserved.
doi:10.1016/j.sna.2005.03.050

voltage [9]. The device operation is explained through the results obtained from a numerical simulation of its internal electrical configuration.

2. Experimental details

2.1. Sensor configuration

The optically addressed color sensor consists on a single or on two stacked p–i–n sensing photodiodes and two semitransparent contacts. Three configurations (#1, #2 and #3) are proposed as it is sketched in Fig. 1a–c. Single (sensor #1) and stacked (sensors #2 and #3) p–i–n structures were deposited by PE-CVD on glass substrates covered with a transparent conductive oxide front contact (TCO). Thermal evaporated back contacts were deposited on the top of the structure and define the active area of the sensor (4 cm × 4 cm). In sensors #1 and #2, the intrinsic layers are based on a-Si:H and the doped layers on a-SiC:H. In sensor #3, the front p–i–n structure (near the front contact) is based on a-SiC:H while in the back p–i–n structure the p doped layer is based on a-SiC:H and the intrinsic and n doped layer on a-Si:H. The structure and geometry of sensors #1, #2 and #3 are, respectively, ZnO/p type a-SiC:H (50 nm)/a-Si:H (500 nm)/n type a-SiC:H (50 nm)/Al; ITO/p type a-SiC:H (20 nm)/ a-Si:H (500 nm)/n type a-SiC:H (20 nm)/p type a-SiC:H (20 nm)/a-Si:H (500 nm)/n type a-Si:H (20 nm)/metal and ITO/p type a-SiC:H (20 nm)/a-SiC:H (200 nm)/n type a-SiC:H (20 nm)/p type a-SiC:H (20 nm)/a-Si:H (500 nm)/n type a-Si:H (20 nm)/ITO.

2.2. Optical characterization

The devices were characterized through the analysis of the photocurrent and spectral response (in the range of 400–800 nm) under different steady-state optical bias ($\lambda_L = 450$, 550 and 650 nm; $\Phi_L = 2\,\mathrm{mW/cm^2}$) and applied voltages ($-6\,\mathrm{V} < V < 2\,\mathrm{V}$). The optical bias was always applied onto the front contact (see Fig. 1).

The light-to-dark sensitivity was defined as the ratio between the photocurrent with and without optical bias, at a given scanner wavelength (λ_S) and *XY* coordinate. As displayed in Fig. 1, for image and color acquisition, the optical image was projected onto the active surface of the sensor and scanned through the same (sensor #1) or opposite sides (sensors #2 and #3) by sequentially detecting scene information at each *XY* coordinates under appropriated electrical bias. The read-out of the photogenerated carriers was performed using a 200 $\mu\mathrm{W/cm^2}$ red (sensors #1 and #3) or green (sensor #2) scanner with a chopper frequency around 1 kHz. The scanner-induced photocurrent is measured using a lock-in amplifier.

3. Results and discussion

The spectral response of the three devices was analyzed in order to determine its dependence on the applied optical/electrical bias. As can be seen from Fig. 2, as the applied voltage changes from negative to positive the spectral sensitivity decreases. Its decay rate depends on the optical bias wavelength and on the device configuration, allowing color recognition in all the analyzed sensors.

In sensor #1, the spectral sensitivity at zero voltage is higher without optical bias and the increase of the read-out voltage causes the spectral response to decrease steeply at a fast rate in dark, and very slowly under red and green illumination. In the stacked structures, the spectral response presents a different behaviour. In dark (without optical bias) it is independent on the applied voltage, remaining constant in the analyzed voltage range. In sensor #2, the spectral sensitivity without optical bias is almost constant and under illumination a strong dependence on the optical bias wavelength with the applied voltage is observed, in the green spectral region. In sensor #3, the spectral response is enhanced without optical bias. Under red optical bias, it is independent on the applied voltage and its magnitude is 10 times less. Under green optical bias the spectral response is smaller than without optical bias, but as the reverse voltage increases it also

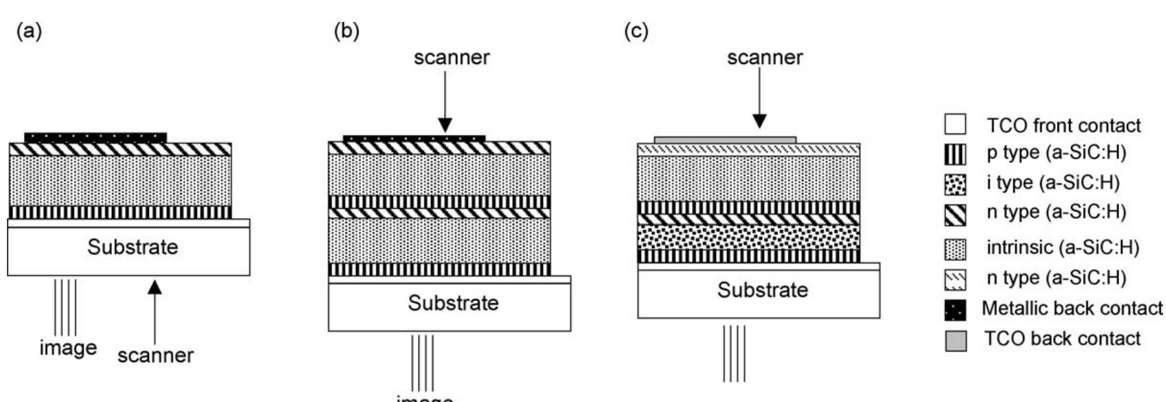

Fig. 1. Schematic structure and read-out of the devices: (a) sensor #1, (b) sensor #2 and (c) sensor #3.

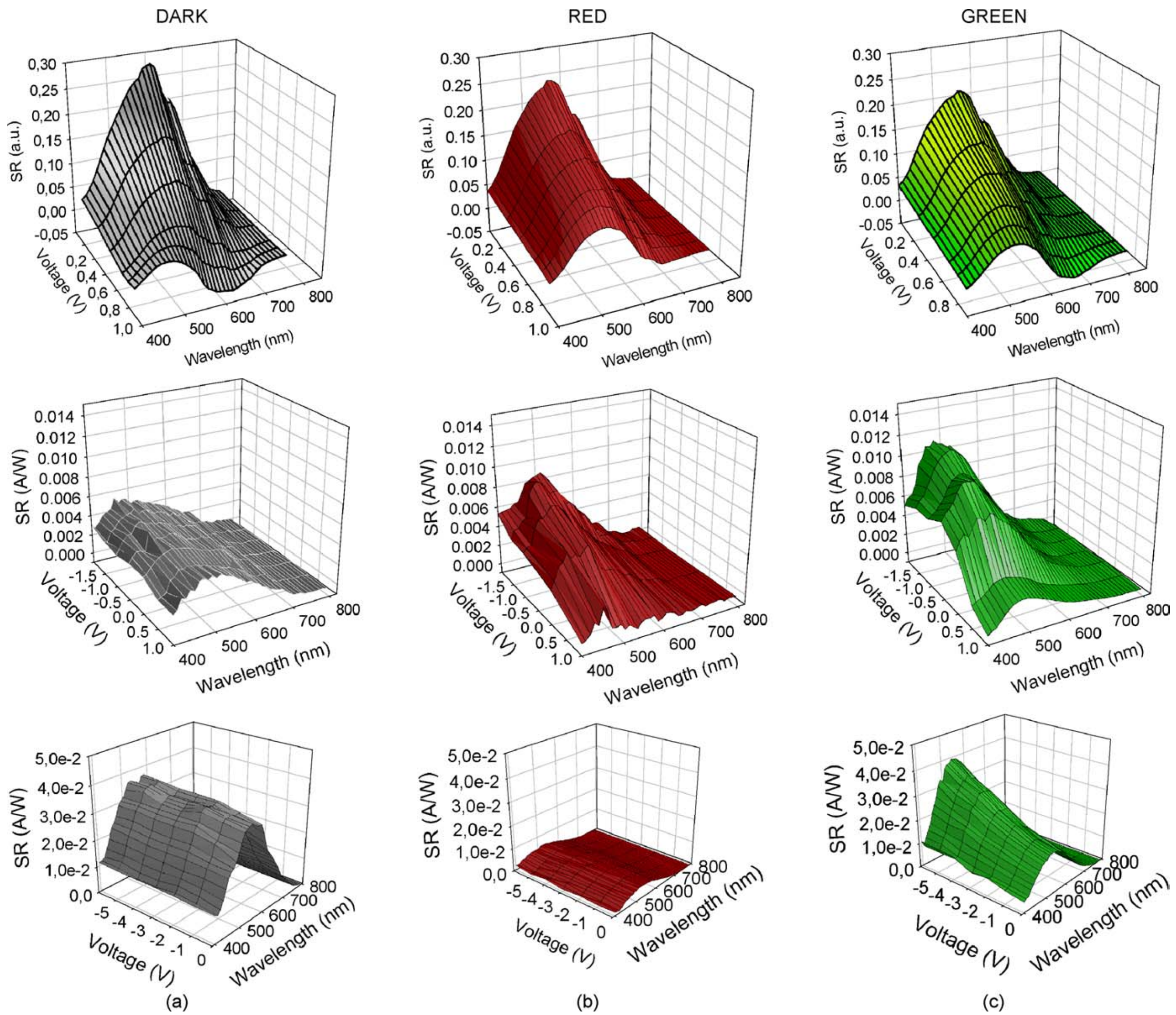

Fig. 2. Responsivitiy dependence on the read-out voltage under steady-state light conditions: (a) in dark and under (b) green (550 nm), (c) red (650 nm), bias and $\Phi_L = 100\ \mu W/cm^2$ for sensor #1 (top), sensor #2 (center) and sensor #3 (bottom).

increases, reaching the same value of the spectral response without optical bias at −6 V.

In Fig. 3 is displayed the collection efficiency as a function of the applied bias in dark ($\Phi_L = 0$) and under steady-state illumination, $\Phi_L = 2\ mW\ cm^{-2}$, at different wavelengths (λ_L) for sensor #1 (a), sensor #2 (b) and sensor #3 (c). Results show that the collection efficiency at an appropriated wavelength (Fig. 2) depends on the optical bias conditions and device configuration (single or stacked), and composition of the front intrinsic layer (with or without carbon). As the applied bias changes from reverse to forward bias the carrier collection decreases, with different slopes in dark and under illumination. This behavior allows light-to-dark sensitivity and enables all the three structures with color sensing properties.

As expected (see Fig. 2) different trends are observed, depending on the device configuration. In sensor #1 as the applied voltage decreases the carrier collection also decreases, in a steep way in dark and more slowly under illumination. For a drift-controlled device, it should be expected a change in sign near the open circuit voltage. However, due to the high resistive doped layers the turn-off in sign shifts to higher values due to the increased flatness of the curves beyond this voltage (Fig. 2). Color information can be extracted (see arrows in Fig. 3a). By tuning the voltage to different values of the forward bias both red and green signals can be successively suppressed, which allows color recognition [10]. In sensor #2, the collection efficiency trend without optical bias is independent of the read-out voltage and cross also the red and green collection curves at different values of the applied

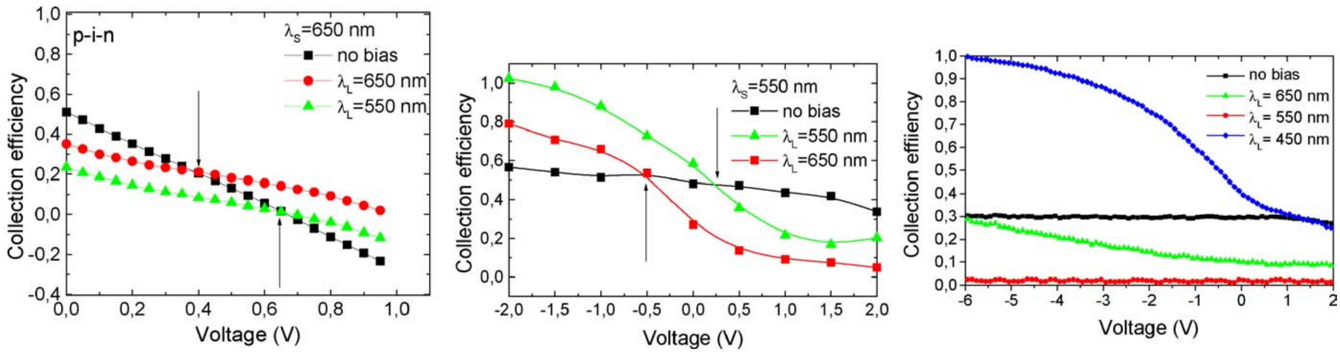

Fig. 3. Collection efficiency in dark and under red and green steady-state illumination for sensor #1 (a), sensor #2 (b) and sensor #3 (c).

bias [9]. In sensor #3, the trend is different as the presence of carbon in the front photodiode light filters the structure. The collection efficiency without optical bias and under red optical bias remains constant in the analyzed voltage range. Under green optical bias the collection efficiency curve intersects the curve without optical bias at −6 V, which allows at this voltage value the possibility of recognizing the red and blue signals. Under forward bias, the blue signal is suppressed around +1 V, which means that at this voltage value both green and red signals can be identified. In this structure, color recognition is obtained by suppressing the blue and the green photocurrent at different values of the applied voltage, which depend on the power density of both image and scanner light. In this structure, the separation of the spectrum in bands is assured by the thin a-SiC:H intrinsic layer of the front photodiode. Its thickness and optical gap (2 eV) were optimized for high conversation efficiency in the blue light and transparency of the red photons coming either from the image (front photodiode) or from the scanner (back photodiode). The conversion efficiency in the blue range is maximized inside the a-SiC:H front diode (200 nm) and in the red range inside the a-SiH back diode (500 nm). The green photons absorption occurs across the front photodiode, the n–p defectous interface and at the front side of the back photodiode (Fig. 1a). Under reverse bias and blue irradiation, the collection is high since the back photodiode becomes fully depleted due to its self-biasing process. Under red illumination, due to the high light penetration depth of the red photons and higher conversion efficiency of the a-Si:H intrinsic layer of the back photodiode acting, as a load (ON state), the collection is almost inexistent. In the green spectral range as the reverse bias increases due to the increase of the potential drop across the switching diode the collection increases linearly. It is interesting to notice that around −6 V the collection with or without green optical image is the same, leading to the rejection of the green images.

4. Sensor operation

To support the image acquisition and representation process we took into account the experimental characterization of the single layers [11] and devices and some results from a computer simulation performed using the ASCA simulator. Details about the program are described elsewhere [12].

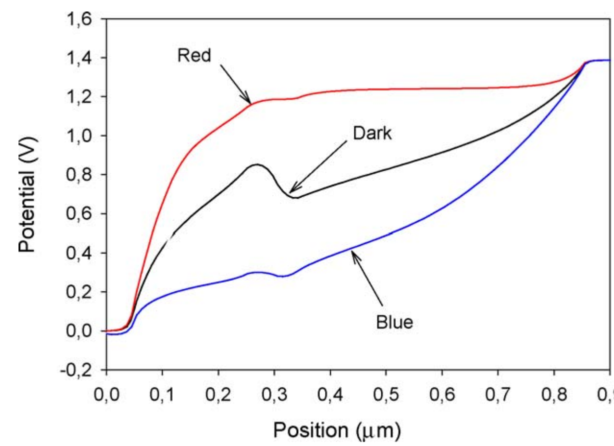

Fig. 4. Simulated potential profiles in short-circuit condition within the structure for different wavelengths of the incident light.

In Fig. 4 it is displayed the simulated potential profiles within sensor #3 for different wavelengths of the incident light (similar data for sensors #1 and #2 can be found in literature [9,10]). Under short circuit condition, the perturbation on the potential profile due to the incident light depends on the wavelength. In all the cases considered, and even under low power radiation, the potential barrier at the internal n–p interface is reduced. In the intrinsic layer of the front photodiode the potential profile becomes flat, while the other photodiode suffers a reverse internal self-biasing to compensate the potential variation. We observe an opposite behavior under low energy radiations (red) and high energy ones (blue), due to the different penetration length of the light.

The photocurrent perturbation read through the LSP technique with a pulsed red laser scanning the back photodiode must be interpreted as a direct dependence of the photocurrent on the incident power light in the case of a red image reading, and as a compensation of the reverse internal self-biasing of the back photodiode when the device is illuminated with a blue image.

Superposition of bias light and external applied bias can cancel out the blue and green photocurrent at a certain value of the applied bias. It is, thus, possible to use this structure as a color recognition device. The main difference from the previous structures is that the identification of color is obtained though the suppression of the blue and green photocurrents, instead of the red and green signals. Further work on the device optimization is still needed, such as reducing the thickness of the internal recombination junction (in order to enhance diffusion transport for red detection) and increasing the intrinsic layer thickness of the back a-Si:H photodiode (in order to obtain a better detection of green color by enhancing the reverse internal self-biasing of the back photodiode).

5. Conclusions

Single and stacked p–i–n structures based on a-SiC:H material were compared and its ability as color sensor analyzed. Results show that the collection efficiency and the light-to-dark sensitivity are dependent on the type of structure (single or stacked), on the composition of the front intrinsic layer, as well as the geometry of the intrinsic layers of the stacked structures and also on the read-out voltage. By tuning the voltage to appropriate values the red, the green or the blue signal can be suppressed allowing color recognition. Combining the signal information at these voltages a color image can be acquired. A numerical simulation supports the sensor operation.

Acknowledgement

This work has been financially supported by POCTI/ESE/38689/2001 project.

References

[1] J.W. Horton, R.V. Mazza, H. Dym, The scanistor: a solid-state image scanner, Proc. IEEE 52 (1964) 1513–1519.
[2] G.F. Amelio, Charge coupled devices, Sci. Am. 230 (1974) 22–31.
[3] T. Neidlinger, R. Bruggemann, H. Brummak, M.B. Schubert, Colour separation in a-Si:H based on p–i–i–n sensors: temperature and image intensity, J. Non-Cryst. Solids 227–230 (1998) 1335–1339.
[4] D. Caputo, G. Cesare, New a-Si:H two terminal switching device for active display, J. Non-Cryst. Solids 198–200 (1996) 1134–1136.
[5] H. Stiebig, M. Böhm, Optimi zation criteria for a-Si:H nipin color sensors, J. Non-Cryst. Solids 164–166 (1993) 785–788.
[6] D. Knipp, H. Stiebig, J. Fölsch, R. Carius, H. Wagner, Improved concept for nipiin and piiin color sensitive two-terminal devices with high linearity, in: Materials Research Society Symposium Proceeding, vol. 467, 1997, p. 931.
[7] M. Vieira, M. Fernandes, J. Martins, P. Louro, A. Maçarico, R. Schwarz, M. Schubert, Laser scanned p–i–n photodiode (LSP) for image detection, IEEE Sens. J. 1 (2) (2001) 158–167.
[8] M. Vieira, M. Fernandes, P. Louro, J. Martins, A. Maçarico, R. Schwarz, M. Schubert, New p–i–n imager configuration for spatial resolution improvement, Sens. Actuators A 92 (2001) 60–66.
[9] P. Louro, M. Vieira, A. Fantoni, M. Fernandes, C. Nunes de Carvalho, G. Lavareda, Large area single and stacked p–i–n photodiodes as color image sensors, in: Materials Research Society Proceeding, vol. 815, S. Francisco, U.S.A., April 12–16, 2004, p. J3.2.
[10] P. Louro, A. Fantoni, Yu. Vygranenko, M. Fernandes, M. Vieira, Analysis of the bias dependent spectral response of a-SiC:H p–i–n photodiode, in: Materials Research Society Symposium Proceeding, vol. 715, S. Francisco, U.S.A., April 1–5, 2002, p. A7.3.
[11] P. Louro, M. Vieira, Y. Vygranenko, M. Fernandes, R. Schwarz, M. Schubert, Bias dependent photocurrent collection in p–i–n a-Si:H/SiC:H heterojunctions, Sens. Actuators A: Phys. 97–98 (2002) 221–226.
[12] A. Fantoni, M. Fernandes, P. Louro, I. Rodrigues, M. Vieira, a-SiC:H tandem photodiodes: a numerical simulation, Sens. Actuators A 113 (3) (2004) 324–328.

Biographies

Paula Louro was born in Portugal in 1967. In 1990, she became researcher in EID Lisbon, Portugal, in the Department of Optoelectronics. She graduated in physics by the Faculty of Sciences from the University of Lisbon in 1990. In 1995, she received the masters of science in material engineering by the New University of Lisbon. Currently, she is assistant professor in the Electronics Department of ISEL, Lisbon, Portugal, where she teaches electronic and semiconductor physics. Her main research interest is in the field of amorphous semiconductor thin films and devices.

Manuela Vieira was born in Lisbon, Portugal. In 1986, she received the masters of science in solid state physics-microelectronic and in 1993 the PhD in semiconductor materials both from the New University of Lisbon. She is full professor in electronics in the Department of Electronics Telecommunication and Computers (ISEL, Portugal) and the head of a group in applied research in microelectronic optoelectronic and sensors—GIAMOS. She has several scientific papers and 20 years of experience in the field of thin films and devices, her research activities have been mainly related to the development of optical sensors.

Alessandro Fantoni was born in Rome (Italy) in 1966. He received a university degree in applied mathematics from the University of Camerino, Italy (1992), and a PhD in material engineering/micro and optoelectronics from the New University of Lisbon, Portugal (1999). He actually teaches semiconductor physics in the Electronics, Telecommunications and Computer Department in the Engineering Institute of Lisbon. His research interests are related to numerical analysis and simulation of micro and optoelectronic thin film devices.

Miguel Fernandes was born in Portugal in 1970. He graduated in physics and materials engineering by the Faculty of Sciences and Technology from the New University of Lisbon in 1995. Currently, he is assistant professor in Electronics Department of ISEL, Lisbon, Portugal, and investigator in the group of applied research in microelectronic optoelectronic and sensors—GIAMOS in the same institution.